sustainability

MDPI

Article

Mechanical Characterization of Industrial Waste Materials as Mineral Fillers in Asphalt Mixes: Integrated Experimental and Machine Learning Analysis

Nitin Tiwari [1,2,*], Nicola Baldo [3,*], Neelima Satyam [2] and Matteo Miani [3]

[1] Lyles School of Civil Engineering, Purdue University, West Lafayette, IN 47907, USA
[2] Department of Civil Engineering, Indian Institute of Technology Indore, Indore 452020, India; neelima.satyam@iiti.ac.in
[3] Polytechnic Department of Engineering and Architecture (DPIA), University of Udine, 33100 Udine, Italy; matteo.miani@phd.units.it
* Correspondence: tiwari50@purdue.edu (N.T.); nicola.baldo@uniud.it (N.B.)

Abstract: In this study, the effect of seven industrial waste materials as mineral fillers in asphalt mixtures was investigated. Silica fume (SF), limestone dust (LSD), stone dust (SD), rice husk ash (RHA), fly ash (FA), brick dust (BD), and marble dust (MD) were used to prepare the asphalt mixtures. The obtained experimental results were compared with ordinary Portland cement (OPC), which is used as a conventional mineral filler. The physical, chemical, and morphological assessment of the fillers was performed to evaluate the suitability of industrial waste to replace the OPC. The volumetric, strength, and durability of the modified asphalt mixes were examined to evaluate their performance. The experimental data have been processed through artificial neural networks (ANNs), using k-fold cross-validation as a resampling method and two different activation functions to develop predictive models of the main mechanical and volumetric parameters. In the current research, the two most relevant parameters investigated are the filler type and the filler content, given that they both greatly affect the asphalt concrete mechanical performance. The asphalt mixes have been optimized by means of the Marshall stability analysis, and after that, for each different filler, the optimum asphalt mixtures were investigated by carrying out Indirect tensile strength, moisture susceptibility, and abrasion loss tests. The moisture sensitivity of the modified asphalt mixtures is within the acceptable limit according to the Indian standard. Asphalt mixes modified with the finest mineral fillers exhibited superior stiffness and cracking resistance. Experimental results show higher moisture resistance in calcium-dominant mineral filler-modified asphalt mixtures. Except for mixes prepared with RHA and MD (4% filler content), all the asphalt mixtures considered in this study show MS values higher than 10 kN, as prescribed by Indian regulations. All the values of the void ratio for each asphalt mix have been observed to range between 3–5%, and MQ results were observed between 2 kN/mm–6 kN/mm, which falls within the acceptable range of the Indian specification. Partly due to implementing a data-augmentation strategy based on interpolation, the ANN modeling was very successful, showing a coefficient of correlation averaged over all output variables equal to 0.9967.

Keywords: recycling; cement; asphalt mixtures; machine learning; data augmentation

Citation: Tiwari, N.; Baldo, N.; Satyam, N.; Miani, M. Mechanical Characterization of Industrial Waste Materials as Mineral Fillers in Asphalt Mixes: Integrated Experimental and Machine Learning Analysis. *Sustainability* **2022**, *14*, 5946. https://doi.org/10.3390/su14105946

Academic Editor: Ali Jamshidi

Received: 5 April 2022
Accepted: 12 May 2022
Published: 13 May 2022

1. Introduction

Rapid growth in society leads to the intensive use of natural resources and further increases waste generation. The disposal of these waste materials is a massive challenge for almost every country. Therefore, the need for sustainable and eco-friendly materials has risen. The researchers are continuously looking forward to exploring sustainable strategies to minimize waste generation and the use of natural resources. Along with 180 other countries, India has signed an agreement under the United Nations (UN) to restrict the average global temperature increase to 1.5 °C (Paris Agreement, 2015) [1]. The UN also

developed the 2030 Agenda for Sustainable Development Goals (SDGs), and SDG-9 and SDG-11 are focused on sustainable and resilient infrastructure and cities (The 17 Goals, Sustainable Development, 2015). In order to achieve SDG-9 and SDG-11, researchers are striving to develop and adopt sustainable practices in infrastructure development by minimizing the use of natural materials in construction, and incorporating industrial waste in construction practices, to reduce the disposal issues [2].

Eco-friendly and durable pavement construction enhances the overall sustainability of smart cities, and it takes a step toward achieving SDG-11. Flexible pavement construction is the most-used pavement system in the world; therefore, any improvement in the asphalt concrete will enhance the overall performance of the flexible pavement structure. The use of industrial waste materials in road pavement construction is an effective way to increase sustainability in the construction industry and minimize waste disposal issues. The use of waste materials in road pavement also reduces the greenhouse gas emissions due to the use of materials such as cement, which is the conventional filler for asphalt concretes in India. Moreover, the recycling of industrial waste materials in pavement construction supports the on-time supply of the required construction aggregates, reduces the consumption of natural resources, and minimizes air, water, and land pollution [3,4]. However, it is imperative to identify suitable replacements for the conventional natural resources in construction without compromising the engineering properties of the modified material.

The effective utilization of industrial wastes to improve the engineering properties of asphalt concretes has been demonstrated by several researchers, in terms of the partial or total replacement of the coarser part of the limestone aggregate structure [5–13]. The largest part of the world's road network (almost 95%) is built with flexible pavements [14]; therefore, the use of waste materials in flexible pavement construction can be more advantageous. The surface layer of any flexible pavement is built with asphalt mixes, which are prepared with aggregates and bitumen. The performance of asphalt concretes depend on the packing of the aggregates and on the adhesion provided by the bitumen [15]. The finest part of the aggregate, also termed a mineral filler, highly influences the mechanical properties and durability of the asphalt concrete [14]. The mineral filler is added to the asphalt concrete for reducing the voids and improving the strength, density, and water resistance. The physico-chemical properties of asphalt mastic (bitumen and mineral filler combination) affect the viscosity of the mixes [3,14]. The various properties of the mineral filler, including shape and size, specific surface area, specific gravity, and chemical composition, are among the most critical parameters that affect the asphalt mixes' overall performance [16,17]. Therefore, an extensive and deep characterization of the industrial waste is required in order to properly optimize the performance of the asphalt mixes.

The conventional mineral filler for asphalt pavements in India is cement; however, its production leads to the emission of greenhouse gases. Therefore, a suitable alternative filler needs to be identified. However, it has to be ensured that the addition of such alternative filler materials does not compromise the performance of the asphalt concrete. Various waste materials such rice dust [18], coal ash [19–21], empty palm fruit bunch ash [22], limestone dust [23], marble dust [19], stone dust [18], brick dust [18,24], bauxite residue [25], rice husk ash [18], and copper slag powder [26] have been investigated as alternative fillers.

It has been observed that some industrial wastes effectively improve the engineering properties of the asphalt mix, and acceptable performances of asphalt mixes have been obtained.

For example, Awed et al. [27] showed that the use of fillers obtained from marble, granite, and steel slag wastes returned technically acceptable mixture performance, with marble being preferable to the other two wastes. In general, according to Hamedi et al. [28], higher amounts of CaO and lower amounts of SiO_2 in the aggregate, for instance, what happens with marble fillers, provide great resistance against moisture-induced damage. Finally, Sherre and Liao [29] have verified that using hollow concrete block powder as a filler, in contrast to brick powder, extends asphalt mixtures' service life by improving their moisture, rutting, and cracking resistance.

The results of such investigations encourage the use of waste materials in flexible pavement construction. In conclusion, the effective use of some waste materials, on one hand, enhances the performance of the asphalt concrete, and on the other hand, reduces waste disposal problems.

Even if several extensive studies have been carried out successfully on individual waste fillers, their use in the field is still very limited. Therefore, a detailed investigation of mixes prepared with various waste fillers is needed to properly evaluate their performance in comparative terms. This study is focused on evaluating the effect of silica fume (SF), limestone dust (LSD), stone dust (SD), rice husk ash (RHA), fly ash (FA), brick dust (BD), and marble dust (MD) as mineral filler in asphalt concrete, and presenting a detailed comparative analysis.

A recent overall trend in evaluating pavement performance and condition is to apply machine learning techniques. In recent years, it has been observed that the performances of support vector machine, random forest, artificial neural network, and deep learning models are sometimes faster and more accurate than the empirical and/or statistical techniques [30,31], providing an alternative to the fundamental, rational constitutive laws of the mechanics of materials [32–35]. Automatic approaches for asphalt pavement crack detection and classification have been established by many authors [36–38], whereas other researchers have focused their efforts on modeling performance in terms of the international roughness index [39,40] or tensile strength ratio and fatigue life ratio [41,42].

For these reasons, the experimental data have been analyzed by means of machine learning techniques, namely, artificial neural networks (ANNs), in order to develop predictive models of the main mechanical and volumetric parameters considered. Predictive equations that can estimate the asphalt mixes' mechanical and volumetric response accurately represent a useful tool to enhance the conventional mix design, based on expensive and time-consuming laboratory tests; in fact, the numerical prediction would allow reducing the number of experiments to optimize the mix, without penalizations in terms of the results' reliability.

The feasibility to fit laboratory data in order to identify predictive equations of the Marshall parameters have already been successfully discussed by Tapkın et al., as well as by Baldo et al. [43,44]. In those studies, large datasets were available. In general, extensive training datasets are needed to properly train the model in order to reduce the over-estimation of out-of-sample results. Nevertheless, most of the time, the available laboratory datasets are quite small, with respect to what is required by conventional neural approaches.

In the present study, a mechanical characterization of seven industrial waste materials used as mineral fillers to improve the performance of asphalt concrete, including silica fume (SF), limestone dust (LSD), stone dust (SD), rice husk ash (RHA), fly ash (FA), brick dust (BD), and marble dust (MD), has been carried out. An integrated experimental and machine learning approach has been used to investigate the effect of the waste mineral fillers on the performance of the asphalt concrete and to develop the prediction model. The experimental analysis has been carried out by conducting the material characterization of each of the seven filler materials. The mechanical performance has been evaluated for asphalt mixes consisting of different proportions of the filler content. Based on a dataset obtained from an experimental investigation, an unconventional approach, namely, the k-fold cross-validation and data augmentation, has been used to properly train the neural network model to maximize its reliability, despite the relatively few experimental data available. This research study has been articulated in three major sections. The industrial waste mineral filler, bitumen, and aggregate material characterization, along with the detailed experimental and machine learning approach, are discussed in Section 2. In-depth results and discussion obtained from the experimental study and ANN analysis are presented in Section 3. The conclusions, obtained from the detailed results and discussion, are mentioned in Section 4, along with the future scope and limitations of this study.

2. Materials and Experimental Investigation

2.1. Materials

This section presents the properties of various materials used in the present research. Detailed physical and chemical characterizations of bitumen, aggregates, and mineral fillers are carried out to analyze the behavior of the materials composing the asphalt concrete. In this study, the utilization of waste materials as a sustainable filler in asphalt mixtures for the base course of road pavements, in substitution of OPC, has been studied. The base course layer has been considered to evaluate the effect of waste materials as mineral fillers for heavy load requirements in the Indian scenario.

2.1.1. Aggregate and Bitumen Properties

Sharp-edged crushed quartz aggregates were used in this study. The material was provided by Safew Tech Systems Indore (India). The various physical aggregates' properties, as per the requisites of the Indian Ministry of Road Transportation and Highway [45], are investigated for the collected samples.

To assess the properties of the aggregates, various laboratory experiments (cleanliness, grain size distribution, bulk specific gravity, Los Angeles abrasion, soundness, shape and flaking, impact strength, and water absorption) have been carried out. The physical properties of the aggregates are shown in Table 1. The grading curve of the aggregate investigated has been compared with the reference envelope prescribed by MoRTH [45] for flexible road pavements, leading to the classification of the material as grade II.

Table 1. Properties of aggregate and bitumen.

Material	Test Parameters	Specified Limit (MoRTH)	Test Results	Test Method
Aggregate	Cleanliness (dust) (%)	Max 5 %	3	IS 2386 Part I
	Bulk specific gravity (g/cm3)	2–3	2.68	IS 2386 Part III
	Percent wear by Los Angeles abrasion (%)	Max 35 %	10.6	IS 2386 Part IV
	Soundness loss by sodium sulphate solution (%)	Max 12%	3.4	IS 2386 Part V
	Soundness loss by magnesium sulphate solution (%)	Max 18%	3.7	IS 2386 Part V
	Flakiness and elongation index (%)	Max 35%		IS 2386 Part I
	20 mm		27.93	
	10 mm		32.13	
	Impact strength (%)	Max 27%		IS 2386 Part IV
	20 mm		4.15	
	10 mm		5.91	
	Water absorption (%)	Max 2%	1.67	IS 2386 Part III
Bitumen	Absolute viscosity at 60 °C (poises)	2400–3600	2855	IS 1206 (P-2)
	Kinematic viscosity at 135 °C (cSt), Min.	350	392	IS 1206 (P-3)
	Flash point Cleveland open cup, (°C), Min.	250	304	IS 1448 (P-69)
	Penetration at 25 °C, 100 gm, 5 sec, (1/10 mm), Min	45	49	IS 1203
	Softening point (R&B), (°C), Min	47	48	IS 1205
	Matter soluble in trichloroethylene, (% by mass), Min.	99	99.45	IS 1216
	Viscosity ratio at 60 °C, Max	4.0	1.3	IS 1206 (P-2)
	Ductility at 25 °C, (cm) after TFOT min.	40	75	IS 1208
	Specific gravity (gm/cc)	0.97–1.02	0.987	IS 1202

Viscosity grade (VG-30) bitumen, conventionally used for road pavement construction in India, has been considered in this research. The used binder is manufactured by Tiki Tar Industries (Vadodara) Limited, Gujarat, India. The various physical properties of the bitumen have been investigated as per Indian standards. The physical properties of the bitumen used in the study are presented in Table 1, along with the MoRTH [45] acceptance requisites.

2.1.2. Mineral Filler

In India, ordinary Portland cement (OPC) is the conventional mineral filler used in the asphalt mix for heavy-load road pavement. To evaluate the effectiveness of the selected waste materials as mineral filler, grade-43 OPC has been used in the study. As per IS 8112-1989 [46], grade-43 OPC has to provide a designed strength of 28 days that is at least equal to 43 MPa. In this analysis, oven-dried filler with a fraction that is finer than 0.075 mm was used. The properties of the waste materials and those of the OPC were assessed by measuring density, specific surface area, and grain size distribution, mineralogical and chemical composition, German filler, and pH value, and conducting methylene blue value analysis. The porosity of fillers was determined as per the German filler test, prescribed by the National Asphalt Pavement Association [47]. The porosity of filler is inversely proportional to its German filler value. The various chemical and physical properties of the fillers are reported in Table 2.

Table 2. Properties of the mineral filler considered.

Property	Type of Mineral Filler							
	OPC	**LSD**	**FA**	**RHA**	**SD**	**MD**	**BPD**	**SF**
Specific gravity (g/cm^3)	3.04	2.65	2.32	2.02	2.69	2.695	2.56	2.2
MBV (g/kg)	3	3.75	3.86	4.72	3.67	4.45	6.25	3.85
German filler (g)	85	97	75	65	85	70	40	94
Fineness modulus (FM)	4.96	3.03	3.77	3.21	5.38	2.12	5.17	1.96
Surface area (m^2/g)	1.75	2.70	2.193	2.31	2.701	4.372	2.688	16.45
pH	12.9	10.22	7.3	10.86	12.57	8.5	8.67	6.98
SiO_2 (%)	21.43	0.48	48.24	89.67	82.37	0.6	39.55	93.5
CaO (%)	66.58	96.57	13.4	1.88	2.79	55.6	12.88	0.89
Al_2O_3(%)	3.01	0.41	24.15	1.62	8.23	0.4	15.71	0.08
MgO(%)	1.39	0.46	1.46	0.97	1.47	0.1	3.29	0.82
Fe_2O_3(%)	4.68	0.32	6.48	1.06	5.27	0.2	14.05	0.5
Particle shape	Granules and sub-angular particles	Granular particles	Rounded	Honeycombed	Angular particles e	Sub-angular	Sub-angular particles	Spherically shaped

2.2. Designing and Testing of Asphalt Concrete

2.2.1. Sample Preparation and Determination of Marshall and Volumetric Properties

Aggregate type, grain size distribution, and bitumen type have been kept constant for all the mixtures investigated in order to assess only the effect of the different filler materials on the physical-mechanical response of the asphalt mixes. Four levels of waste mineral filler have been considered, namely, 4.0%, 5.5%, 7.0%, and 8.5%, by volume of mix; OPC has been used with the same contents as a comparative term. The optimum binder content has been evaluated for each asphalt mixture. The detailed methodology used in this research is shown in Figure 1.

Aggregate, RSH, BPD, MD, SD, FA, LSD, SF, OPC, and bitumen were separately pre-heated at 150 °C for mixing. Dry samples of the required amount of aggregate and fillers were initially mixed at 170 °C in a planetary mixer with a speed of 140 ± 5 rpm; hereafter, varying percentages of bitumen were added for the preparation of the asphalt mixture specimens, according to the Indian MoRTH regulations. Complete laboratory work has been conducted on three replicates, and experimental results are reported with standard deviation.

The Marshall method, based on the impulsive compaction principle, has been used to prepare the specimens for the subsequent physical-mechanical tests. With respect to other laboratory techniques, such as, for instance, the gyratory compaction widely used in the USA within the SUPERPAVE method (NAPA, 1995), the Marshall compaction leads to volumetric properties of the compacted specimens that are quite different from those

observed in road pavement as a result of the rollers' compaction [48]. However, the Marshall compaction is still widely used in many road laboratories [49–54] due to its simplicity, low cost, and extensive database available in the literature.

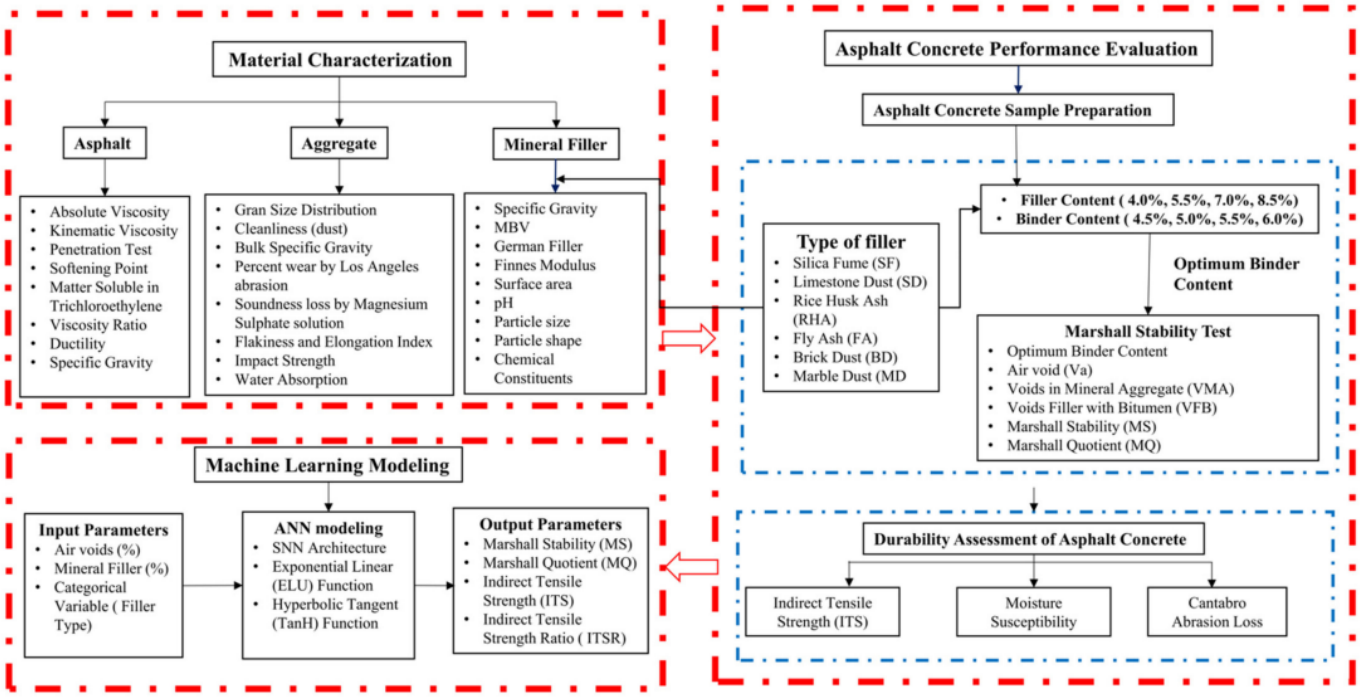

Figure 1. Detailed research methodology used in this research.

Cylindrical specimens of 67 ± 3 mm thickness and 102 mm diameter were compacted by means of a Marshall hammer with 75 blows per side of the specimens, then air-dried for 4 h after compaction, and finally, kept in a water bath at 60 ± 1 °C for 35 ± 5 min prior to the Marshall testing [55]. Three specimens of each type of mix were prepared to investigate the effect of repeatability, and the mean results have been computed along with the standard deviation. A load cell of 100 kN and a 50 mm LVDT with a data acquisition system were used to measure and record the maximum load resistance and respective deformations at a constant strain rate of 50.4 mm/min. The results of the experiments have been reported as Marshall's stability, flow, and quotient.

The volumetric properties are related to the volume of the binder, the mineral filler, and the coarse-aggregates necessary to produce an asphalt mixture of desirable physical and mechanical characteristics. Actually, the volumetric properties of the asphalt mixtures significantly affect the strength and long-term durability of a road pavement. The various volumetric properties, which include maximum theoretical specific gravity, dry density, percentage of air voids (Vv), voids in mineral filler, and voids filled with bitumen, have been determined according to the relevant standards specified by the Indian Ministry of Road Transport and Highways (MoRTH) [45]. The details of the testing equipment used in this study are tabulated in Table 3.

Table 3. Specifications of the equipment used for testing.

No.	Name of Equipment	Specification
1.	Digital Marshall Stability Apparatus	Ref. standards—ASTMD 1559, ASTM D6927-06 Capacity—100 kN single speed Sample size—4″ and 6″ dia Load cell: 100 kN LVDT: 50 mm Maximum vertical clearance—470 mm Minimum vertical clearance—250 mm Horizontal clearance—265 mm Platen diameter—133 mm Platen travel—25 mm Platen speed—50.8 mm/min Rated power—375 W Dimension (l × w × h)—550 × 400 × 870 mm
2.	Automatic Compactor for Bituminous Mixes	Ref. standards: ASTM D 5581:1996, ASTM D 6926-04 Weight of hammer—4.5 kg (4″ sample dia) and 10.2 kg (6″sample dia) Sample ejector: 4″ and 6″ sample dia Falling height: 457 mm Suitable for operation—440 V and 50 Hz Power supply—three-phase AC supply
3.	Indirect Tensile Strength Test Machine	Ref. standard: ASTM D6931 Ram stroke—400 mm Ram speed range—50 to 70 mm/min Load cell—250 kN Deformation transducer—400 mm Clearance between columns—530 mm Electrical supply—three-phase 415 Volts 50 Hz Dimensions (W × D × H)—2100 × 616 × 2111 mm Working space required (W × D × H)—2300 × 1616 × 2300 mm
4	Los Angeles Abrasion Machine	Ref. Standard: AASHTO T 96, ASTM C535 Revolutions per minute—30–33 Drum diameter—700 mm Inside height—500 mm Electrical—220 V/50 Hz Product dimensions (W × D × H)—965 × 1016 × 1181 mm

2.2.2. Rutting Resistance

The asphalt concrete's rutting performance is empirically correlated with the Marshall quotient (MQ) parameter of the mix [56]. The MQ of the waste-modified and conventional asphalt concrete has been calculated as the ratio between the Marshall stability and flow. A higher MQ value indicates a stiffer asphalt mix, which can perform adequately with respect to permanent deformations due to the traffic load. The higher resistance to creep deformation is offered with the more stiffened asphalt mix. The waste-modified asphalt mixes have been prepared with three replicas (a total 24 samples for 8 fillers) to assess the asphalt mix's performance.

2.2.3. Cracking Resistance

The cracking resistance of AN asphalt concrete can be empirically estimated by means of the indirect tensile strength (ITS) test results. Therefore, for all the mixes investigated, its tests have been carried out as per ASTM D 6931 at 25 °C temperature [57]. The specimens have been prepared according to the protocol used for the preparation of the Marshall specimens. A constant loading rate of 50.8 mm/min has been applied on each Marshall specimen on its diameter in compression. The waste-modified asphalt mixes have been prepared with three replicas (a total 24 samples for 8 fillers) to assess the asphalt mix's performance.

2.2.4. Moisture Susceptibility

Water sensitivity (WS) was evaluated by means of a modified Lottman test [58]. The indirect tensile strength ratio (ITSR) has been computed as the ratio between the ITS values determined before and after moisture conditioning, with the latter carried out according to AASHTO T-283 [59]. Cylindrical specimens of 63.5 mm thickness and 150 mm diameter were prepared by Marshall hammer, with a target air voids content equal to 7 ± 0.5%. The compacted specimens have been stored at room temperature for 24 ± 3 h before moisture conditioning. The specimens were saturated for 10 min at 50 kPa absolute vacuum pressure and then left submerged for an additional 10 min in a vacuum container. The target degree of saturation of the cured specimens was 75 ± 5%. The cured specimens were covered using thin plastic film and sealed in a plastic bag having 10 ± 0.5 mL water. After that, the sealed specimens were placed for freezing at −18 ± 3 °C for 24 h. Subsequently, the frozen specimens were removed from the plastic bag and placed in a water bath for 24 h at 25 ± 5 °C. After the conditioning of the specimens, their indirect tensile strengths were investigated in accordance with ASTM D6931 [57].

2.2.5. Cantabro Abrasion Loss Test

The Cantabro abrasion loss test was carried out to investigate the degradation behavior of the asphalt mix in accordance with [60]. The cylindrical specimens of 50.8 ± 1.5 mm thickness and 101.6 ± 1.5 mm diameter were compacted with 50 blows per side of the specimens using the Marshall compactor. The initial mass (m_i) of the prepared AM has been noted at room temperature (25 °C). After 24 h, the compacted AM specimen was placed in the 700 mm diameter cylinder of the Los Angeles abrasion test machine (500 mm inside height). The test was conducted by removing the metal balls from the cylinder and applying 300 revolutions at 32 rmp speed. Loose material from the specimen was removed and the final mass (m_f) of the broken specimen was noted. The loss in mass was calculated using Equation (1):

$$CL = \frac{m_i - m_f}{m_i} \times 100 \quad (1)$$

where CL is the Cantabro loss percentage, m_i is the initial weight of the test specimen, and m_f is the final weight of the test specimen.

2.3. Theory of Machine Learning Modeling

2.3.1. Artificial and Shallow Neural Networks

Artificial neural networks (ANNs) are optimization algorithms built on the idea of the brain's functioning, and that can be classified as non-linear parametric functions [61,62]. Such networks are usually represented by layered structures composed of elementary units called neurons. All the neurons belonging to the first layer constitute the input layer; those belonging to the last layer constitute the output layer, and all the intermediate layers are called hidden layers. The connections between the layers are total and in only one direction: each unit receives a signal from all the units of the previous layer and transmits its own output value, opportunely weighted, to all the units of the next layer. This output value, commonly called "activity", is defined on the basis of a typically non-linear activation function that characterizes each neuron. These functions generate the neuron's response signal, which usually varies in the range $(0, 1)$ or $(-1, 1)$, as well as $(0,$ infinity$)$ or $(-1,$ infinity$)$, which can be interpreted as a yes/no answer about whether information needs to be transmitted. Everything is aimed at deriving an analytical relationship between the input features and the target variables. In fact, by means of supervised learning algorithms, the network is able to adjust the weights and biases of each connection in order to minimize the prediction errors on the experimental targets.

This study implements an ANN with a single hidden layer: this particular architecture is called a shallow neural network (SNN), and it has been demonstrated that it is possible to solve almost all the multidimensional input-target fitting problems by providing the hidden layer with a sufficient number of neurons [63]. Therefore, information goes from the

input layer to the output layer, passing through one hidden layer. Specifically, the proposed SNN consists of a $3 - N - 4$ architecture (Figure 2); it is composed of 3 neurons in the input layer (the components of the input features vector), N neurons in the hidden layer (with N a variable integer in the range $1 \div 50$), and 4 neurons in the output layer (2 empirical and 2 rational mechanical parameters of asphalt concretes). Moreover, the best activation function for the hidden layer was searched among two different non-linear functions φ: the hyperbolic tangent (TanH) and the exponential linear (ELU) (Figure 3). The former is the most widely used when dealing with input-target fitting problems, whereas the latter has proved to be very successful in image classification and deep learning applications (although it is still seldom used in fitting problems). The output layer was associated with a simple linear activation function. To identify the proper number of neurons and the activation function that produced the best prediction performance on a statistical metric, a grid search was performed, which consists of training all the models defined by the possible pairs $(N,\ \varphi)$ and testing their generalization capabilities.

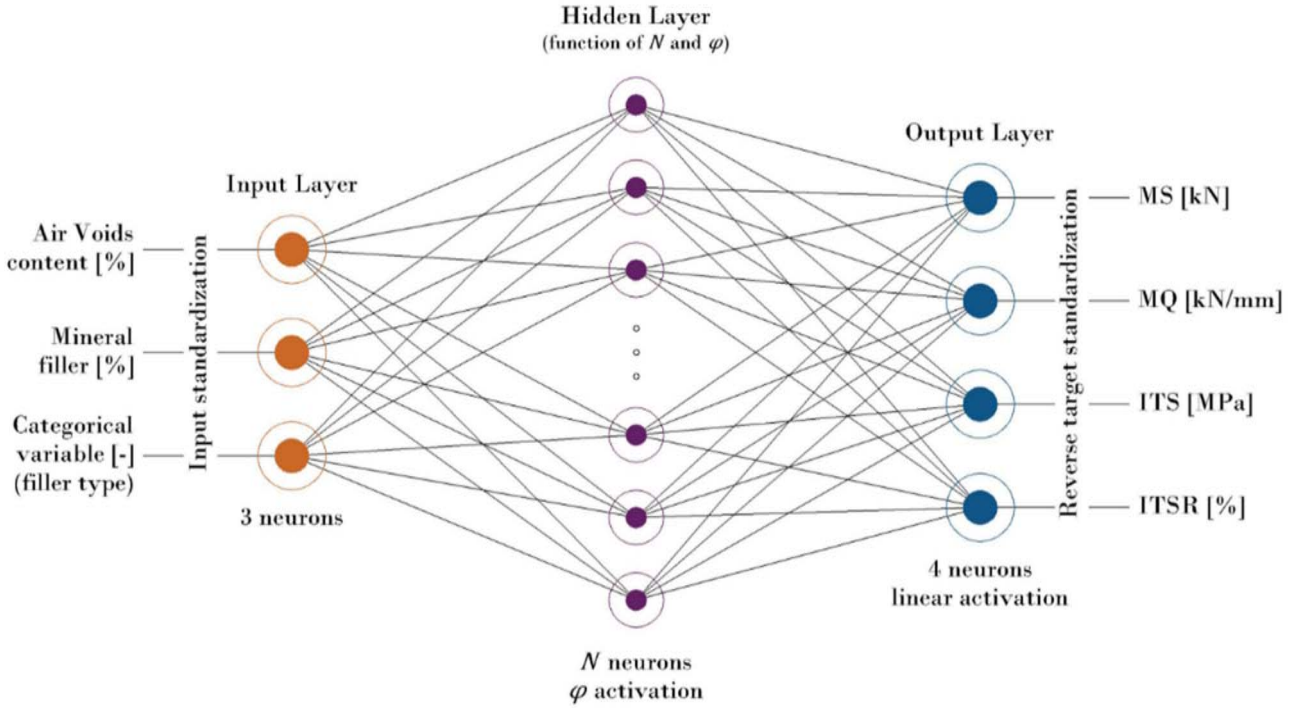

Figure 2. SNN structure diagram.

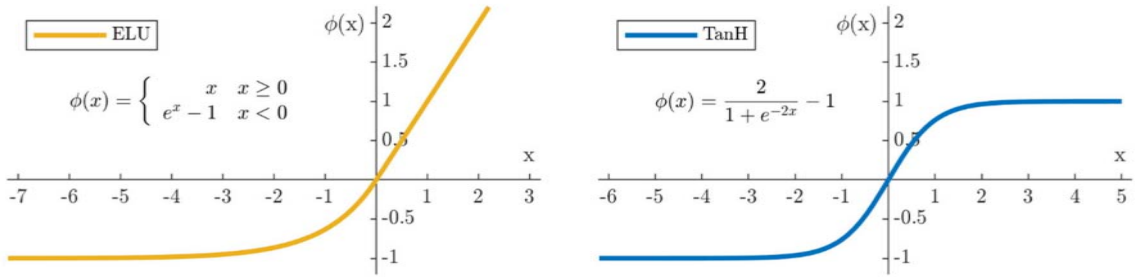

Figure 3. Exponential linear (ELU) and hyperbolic tangent (TanH) activation functions.

The variables used as inputs were the air void contents of each sample, the respective filler percentages, and a categorical variable that accounted for the 8 different filler-types. As is well-known in the asphalt technology, filler type and content greatly affect the mechanical properties of any asphalt mixture; therefore, in the current research paper, both the filler

type and content have been considered as the two major parameters. It can be noticed that the input layer of the proposed SNN has a neuron for each input feature. The target variables, predicted all at once, are the Marshall stability (kN) and the Marshall quotient (kN/mm) (two empirical mechanical parameters from the Marshall test), along with the indirect tensile strength (MPa) and the indirect tensile strength ratio (%) (two rational mechanical characteristics). Finally, in order to allow the model training algorithm to be optimally performed and, at the same time, the computational times to be reduced, both the input and output variables have been standardized before being inputted to the network, so that they had zero mean and unitary standard deviation.

2.3.2. SNN Optimization

The series of sequential steps aimed at identifying the best values of the interneural connections weights and biases is called the learning phase. Since the input/output pairs are available, this process becomes supervised and is divided into two distinct phases: the first is the "forward step", in which the feature input vector $\boldsymbol{x}$ is assigned to the network in order to predict the output vector $\hat{\boldsymbol{y}}$; the second is the "backward step", in which the target vector $\boldsymbol{y}$ is compared with its prediction $\hat{\boldsymbol{y}}$. From the comparison between $\hat{\boldsymbol{y}}$ and $\boldsymbol{y}$, it is possible to define a function $F(\hat{\boldsymbol{y}}, \boldsymbol{y})$, commonly called the performance function or the loss function, which helps with determining the adjustments to be made to the weights and biases matrix $\boldsymbol{W}$, so that a subsequent iteration can produce better results. These adjustments are indicated with the name of learning rule. The analytical expression of the one employed in this study is the following:

$$\boldsymbol{W}^{e+1} = \boldsymbol{W}^{e} - \left(\nabla^2 F(\boldsymbol{W}^{e})\right)^{-1} \nabla F(\boldsymbol{W}^{e}),\ e \in \{1, \cdots, E\} \tag{2}$$

where E is the total number of iterations, and the superscript e stands for the e-th iteration, whereas the notations ∇^2 and ∇ represent the Laplacian and gradient operators, respectively. Assuming a particular type of backpropagation algorithm, also called Levenberg–Marquardt (L.M.) [64], the previous equation becomes:

$$\begin{gathered} \boldsymbol{W}^{e+1} = \boldsymbol{W}^{e} - \left[\boldsymbol{J}^{T}(\boldsymbol{W}^{e})\boldsymbol{J}(\boldsymbol{W}^{e}) + \mu_{\mathrm{e}}\boldsymbol{I}\right]^{-1} \boldsymbol{J}^{T}(\boldsymbol{W}^{e})\boldsymbol{v}(\boldsymbol{W}^{e}),\ e \in \{1, \cdots, E\} \\ \boldsymbol{v}(\boldsymbol{W}^{e}) = \hat{\boldsymbol{y}}(\boldsymbol{W}^{e}) - \boldsymbol{y} \end{gathered} \tag{3}$$

in which $\boldsymbol{W}$ is the weights and biases matrix, $\boldsymbol{J}$ is the Jacobian matrix of the loss function $F(\cdot)$ with respect to $\boldsymbol{W}$, μ is a scalar related to the learning rate, I is the identity matrix, and v represents the vector of the errors made by the network. The scalar μ is also an indicator of the algorithm convergence rate. In fact, whereas the direction to reach the absolute minimum of the loss function is identified by the gradient $\boldsymbol{J}^{T}(\boldsymbol{W}^{e})\boldsymbol{v}(\boldsymbol{W}^{e})$, the size of the step to be taken in such a direction depends on the value assumed by μ. A high value involves a small step, but consequently, the computational time is increased. On the other hand, a low value implies a large step, and despite the lower computational time, could cause a jump over the minimum. For this reason, to avoid both losing the absolute minimum and excessive computational times, three additional hyperparameters (μ_{inc}, μ_{dec}, and $\mu_{\max}$) are introduced. μ_{inc} is a scalar > 1 that multiplies μ_{e} if the performance index between iterations $e-1$ and e is improved. Similarly, if the performance index has worsened, μ_{e} is multiplied by $\mu_{\mathrm{dec}} < 1$. Finally, if the value of μ_{e} becomes too large (greater than $\mu_{\max}$), the LM algorithm is terminated. At the end of the algorithm (either because the maximum number of iterations E or the $\mu_{\max}$ value has been reached), the best weights and biases are kept fixed, and the test feature vector is processed in order to determine the performance metrics on data never before processed. However, under the conditions outlined, there is still the possibility of running into a problem known in machine learning as overfitting. In fact, the neural model could adapt too much to the training dataset and return very poor performance during a testing phase. For this reason, the so-called Bayesian regularization has been introduced [63]. It consists in modifying the loss function $F(\cdot)$ by adding a term

that penalizes networks characterized by high values of connection weights (which cause overfitting problems) and, thus, encourages smoother data regressions. The modified loss function becomes:

$$F_{opt}(\hat{\boldsymbol{y}}(\boldsymbol{W}^e), \boldsymbol{y}, \boldsymbol{W}^e) = \beta \|\boldsymbol{v}(\boldsymbol{W}^e)\|_2^2 + \alpha \|\boldsymbol{W}^e\|_2^2 \quad (4)$$

The regularized loss function is the sum of the 2-norm of the network errors and parameters, multiplied, respectively, by the scalars β and α, whose ratio α/β is in the range $[0, 1]$. When this ratio is too small, it is still possible for the network to overfit. On the other hand, a too-large value of α/β causes the underfitting (the opposite problem) that is a too-smooth interpolation of the training set data. In order to optimize the regularization parameters, David MacKay's approach has been implemented [65], which provides an automatic re-evaluation of α and β for each iteration with the goal of keeping small weights and, at the same time, identifying the loss function's absolute minimum. Regarding the values to be assigned to the hyperparameters of the LM algorithm, it was decided to implement them as defined within the MATLAB® ANN Toolbox. In fact, E has been set equal to 1000, μ_{inc} to 10, μ_{dec} to 0.1, μ_{max} to 1.0e+10, and the starting μ equal to 0.001.

2.3.3. k-Fold Cross-Validation

In order to generate a model from a given dataset, this has to be partitioned in at least two subsets: one that will be used during the training phase, and one in the testing phase. Such practice is known as the hold-out method, and consists of subdividing the available dataset into two random subsets containing a different percentage of data (typically 75% for training and the remaining 25% for testing). This approach often results in biased performance, as subsets may not be well representative of the entire dataset, and some information may, for example, be excluded from the training set. Such an effect becomes more pronounced in smaller datasets [66]. To avoid the problems of the hold-out method, a data-partitioning technique called k-fold cross-validation (CV) was implemented in this paper. This is an iterative technique that consists in defining a number k of partitions: each partition contains the same number of data, so that each of them can be used once in testing and $k-1$ times in training. This process is repeated k times and, for each iteration, a performance metric of the individual model (e.g., the mean squared error) is recorded. The overall performance will be calculated as an arithmetic average of the individual metrics.

$$\begin{aligned} MSE_i &= \|\hat{\boldsymbol{y}}_i - \boldsymbol{y}_i\|_2^2 \\ MSE_{CV} &= \frac{1}{k} \sum_{i=1}^{k} MSE_i \end{aligned} \quad (5)$$

In this way, the results are less affected by performance estimation bias due to data hold-out splitting [67]. In the current study setup, the value of k was set as equal to 4 and the partitioning was of the "stratified" type, so that all the 4 test folds contained one experimentally observed datum for each of the 8 filler types.

During the grid search, it was necessary to define a method to choose the best among the investigated network architectures. Particular attention was paid to the computational efficiency of the model. A model trained through the Bayesian regularization algorithm, thanks to the structure of the algorithm itself, hardly overfits (even for complex architectures with a high number of neurons). However, the more neurons that characterize the hidden layer, the greater the number of weights and biases that must be calculated. In addition, it is possible that some of these parameters do not contribute to reducing performance errors, as they have been set to small values, or even to zero, by the training algorithm. For this purpose, the effective number of parameters (ENP) variable was calculated. It consists of determining the ratio between how many weights and biases within the neural model are actually employed in reducing the loss function [63] and the total number of parameters δ_i in the network. Therefore, in order to find the network that is computationally more

convenient, the difference between ENP and the averaged MSE of the 4 fitted models was maximized:

$$\begin{gathered} L_{CV} = ENP - MSE_{CV} = \sum_{i=1}^{4} \frac{\delta_i - 2\alpha_i \mathrm{tr}\left(\nabla^2 F(\boldsymbol{W}_i)\right)^{-1}}{\delta_i} - \sum_{i=1}^{4} \|\hat{\boldsymbol{y}}_i(\boldsymbol{W}_i) - \boldsymbol{y}_i\|_2^2 \\ \{N,\ \varphi\}_{best} = \underset{(N,\ \varphi)\ \in\ (X_N, X_\varphi)}{\arg\max} \quad L_{CV}(N,\ \varphi) \end{gathered} \tag{6}$$

where $\boldsymbol{W}_i$ is the weights and biases matrix of the i-th SNN trained in the k-fold cross-validation, δ_i is the total number of weights and biases of the same i-th SNN, while α_i and β_i are the regularization terms that can be computed as explained in Hagan et al. [63].

2.3.4. Data Augmentation

In the field of machine learning, the performance of a model often improves as the size of the dataset used to train it increases. For this reason, when dealing with small datasets, it is becoming common practice to use mathematical techniques to increase the amount of data available without having to perform additional expensive experimental campaigns. Such techniques are called data augmentation strategies. Nevertheless, the generated synthetic data have to keep the original meaning of the experimental data [67]. Although this condition is easy to satisfy for image classification (rotating, cutting, or flipping an image does not alter its meaning), such a condition becomes trickier with time-series data forecasting or with input-target fitting problems.

In general, the modeling of real-world problems would require large datasets that collect information about all the correlated features parameters. However, in the context of asphalt pavement engineering, experimental investigations are often limited to analyzing the mechanical behavior (or evaluating the volumetric properties) of only a few variations of a specific asphalt concrete, due to the implicit cost and time of laboratory testing. In this study, given the efforts in preparing multiple Marshall specimens with different bitumen/filler contents, the training set was augmented using an emerging technique in input-target fitting problems [67]: the modified Akima cubic Hermite interpolation, also called "MAKIMA". Such an interpolation method is capable of considering the strong nonlinearity of the problem, but at the same time, avoids excessive fluctuations of the data. The MAKIMA technique represents an improvement of the Akima algorithm [66], and it is easy to be implemented in MATLAB®: it consists in performing a cubic interpolation that produces piecewise polynomials characterized by continuous first-order derivatives. In other words, a generic piecewise cubic polynomial $P(q)$ with $q \in (q_m, q_{m+1})$, an interval of input nodes q to which correspond the values p of the function to be interpolated, has to satisfy the following four interpolation conditions, two on the function values and two on the (unknown) derivative values:

$$P(q_m) = p_m,\ \ P(q_{m+1}) = p_{m+1},\ \ P'(q_m) = d_m,\ \ P'(q_{m+1}) = d_{m+1} \tag{7}$$

where d_m and d_{m+1} are the first derivative values (the slope of the interpolant) at sample points q_m and q_{m+1}. Therefore, the key to the MAKIMA interpolation is the choice of derivatives, which are defined as the weighted average of nearby interval slopes; for example, if $\rho_m = (p_{m+1} - p_m)/(q_{m+1} - q_m)$ is the slope on the interval (q_m, q_{m+1}) and $\rho_{m-1} = (p_m - p_{m-1})/(q_m - q_{m-1})$ is that on the interval (q_{m-1}, q_m), then the Akima derivative value at q_m can be computed locally as:

$$d_m = \frac{\omega_1}{\omega_1 + \omega_2}\rho_{m-1} + \frac{\omega_2}{\omega_1 + \omega_2}\rho_m \tag{8}$$

in which the weights ω_1 and ω_2, used in the modified algorithm, are:

$$\omega_1 = |\rho_{m+1} - \rho_m| + \frac{|\rho_{m+1} + \rho_m|}{2},\ \ \omega_2 = |\rho_{m-1} - \rho_{m-2}| + \frac{|\rho_{m-1} + \rho_{m-2}|}{2} \tag{9}$$

This particular definition reduces, in practice, the number and the amplitude of undulations (or wiggles) of the interpolant with respect to "splines" that, otherwise, compute derivatives by imposing the constraint of continuous second derivatives [66].

As recommended in Oh et al. [67], the augmented data should not outnumber the amount of data in the original dataset. Given that the experimental investigation has considered 4 different filler contents, from 4.0 to 8.5% at step 1.5%, for each of the 8 fillers (the entire dataset counts 32 items), data augmentation aimed at identifying the target values and the air voids corresponding to 0.75% increases incrementally with the filler content (the experimental filler intervals were each divided into two sub-intervals of range 0.75%). Therefore, the size of the augmented dataset was nearly doubled, going from 32 to 56 items (which is also the dimension of the input feature vector). In particular, the MAKIMA technique was applied on the entire experimental dataset, considering, for each type of mineral, filler content increments as nodes, whereas target variables and air voids, taken one at a time, were considered as values to be interpolated. All data obtained by means of MAKIMA augmentation were used exclusively for training the SNN.

Figure 4 graphically shows the feature space points that were considered in the training process: experimentally sampled data are represented by black plus sign markers, whereas the augmented data are represented by red crosses. Furthermore, the curves represented in Figure 4 are the result of MAKIMA interpolations between the filler content and air voids for each of the 8 filler types: the SNNs that were developed in this study admit solutions only along these curves, which reflect the univocal relationship existing between the two main feature variables. In fact, as the type and content of bitumen, as well as the type of coarse aggregate, have been kept constant in the preparation of the investigated mixtures, the increase in the filler percentage by volume of the mix has to be reflected in a reduction of the mixture's air voids content; therefore, this physically observable behavior was properly kept by the MAKIMA interpolation.

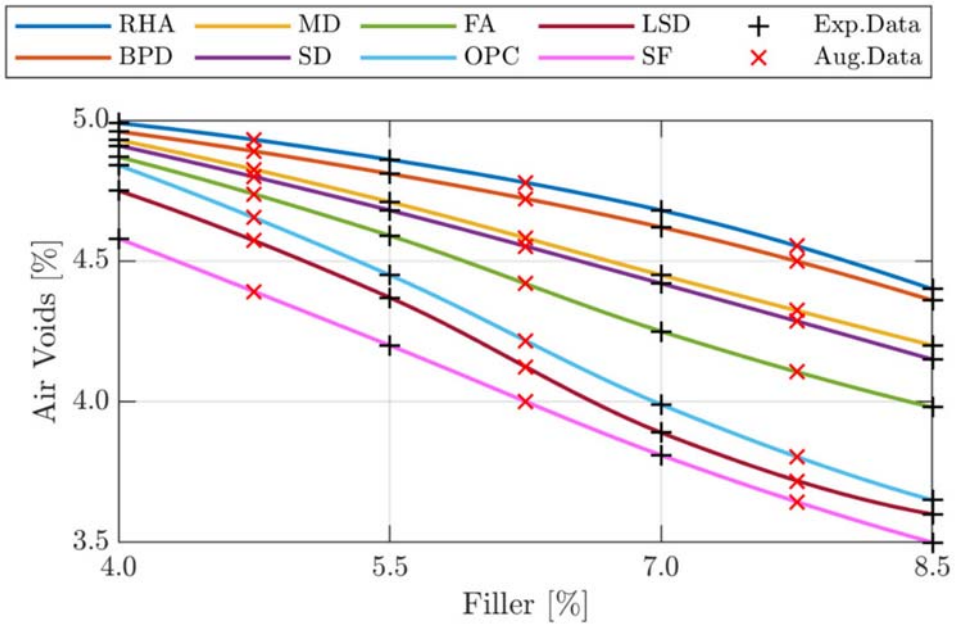

Figure 4. Experimental sampled data (black plus marker) and augmented data (red cross marker).

3. Results and Discussion

3.1. Performance of Modified Asphalt Mixes

The mechanical performance of the investigated asphalt concretes with varying filler contents is discussed in this section.

3.1.1. Marshall and Volumetric Properties

The volumetric properties of the asphalt mixes with waste and conventional mineral fillers are shown in Figure 5. As was expected, for each bitumen content, the higher the filler percentage, the lower the air voids; this result was verified for all asphalt mixes. The air voids' reduction significantly depends on the fineness modulus of the mineral filler.

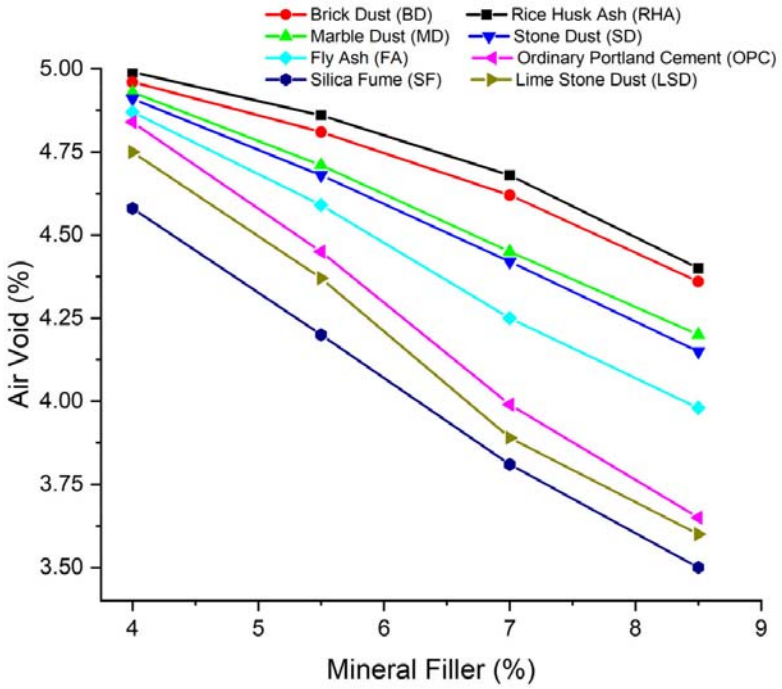

Figure 5. Volumetric properties of the asphalt mixes with waste and conventional mineral fillers.

It can be noted that SF and LSD have a higher FM than the conventional mineral filler OPC; therefore, a higher reduction in the air voids has been observed. The BD has a lower FM, and therefore, less reduction in the air voids. MD and SD have almost similar behaviors. Similarly, BPD and RHA show the same trends. However, all asphalt mixes presented air voids within the acceptable range of 3–5%, as per the Indian Standard.

Voids in the mineral aggregate (VMA) are given by the volume of the intergranular voids between the aggregate particles of a compacted asphalt mixture, including the air voids and the volume of the bitumen not absorbed by the aggregates (Figure 6). Mixes prepared with RHA (16.24%), BD (16.41%), MD (16.31%), SD (16.278%), and FA (15.99%) also had higher VMA than OPC (15.87%), LSD (15.74%), and SF (15.52%) mixes at 8.5% mineral filler content. Hence, a higher porosity of filler could increase the absorbance of bitumen in its mix.

Voids filled with bitumen (VFB) are termed as the percentage of VMAs that is occupied by bitumen. As a consequence of the air voids and VMA values previously determined, mixes with SF (77.44%) and LSD (77.16%) had slightly higher VFB values with respect to the asphalt mixtures made with OPC (77.01%), as shown in Figure 7. The values of VFB for FA (75.10%), SD (74.49%), MD (74.27%), BD (73.45), and RHA (72.80) are lower than the conventional filler OPC (77.01%) at 8.5% mineral filler content. Hence, these materials can be preferred as fillers in regions with hot climates [68] due to their lower bleeding possibilities. It can be also observed that the value of VFB has been increased with the increase in the filler content. All the asphalt mixtures considered presented VFB values within the range 65–85%, as prescribed by Indian regulations [45].

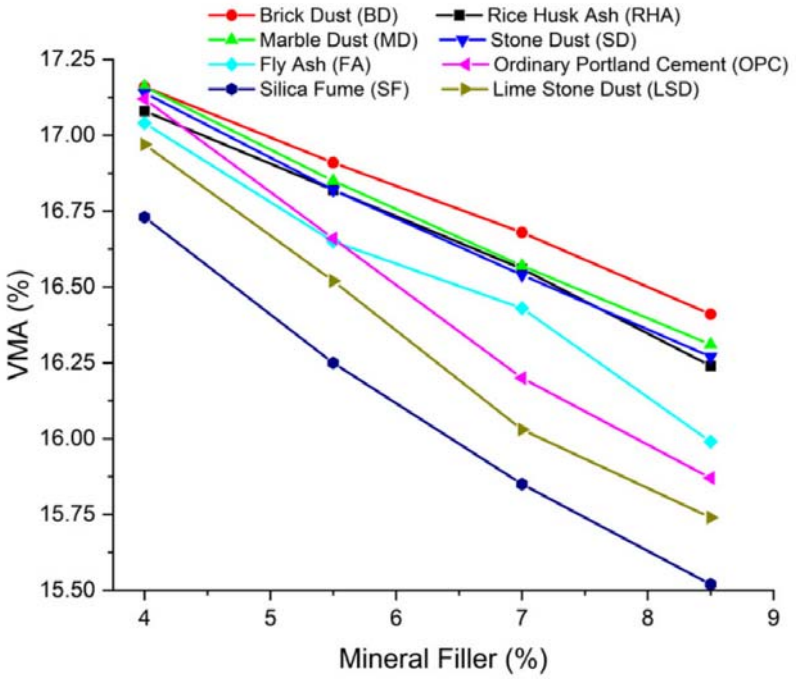

Figure 6. Voids in the mineral aggregate of the asphalt mixes with waste and conventional mineral fillers.

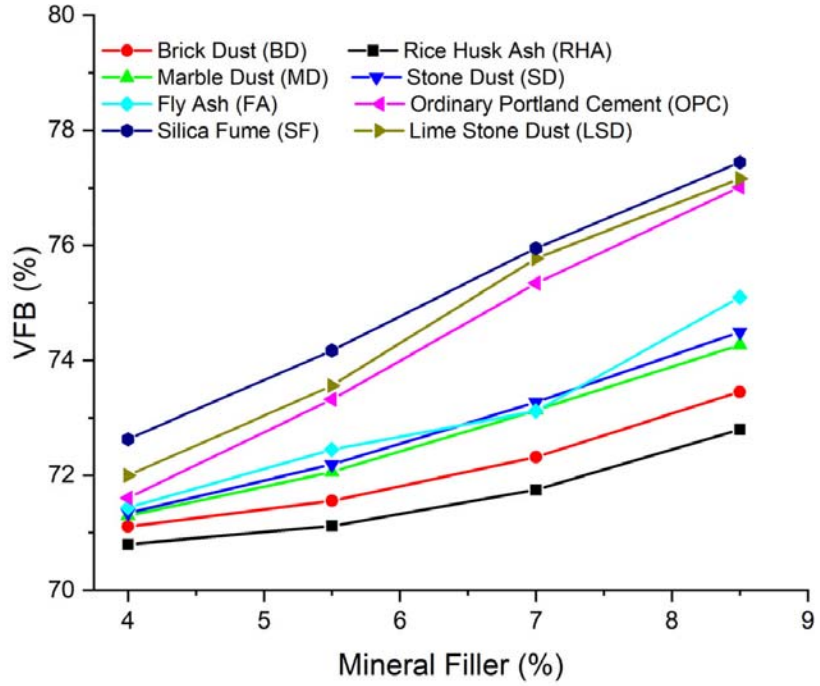

Figure 7. Voids filled with bitumen of the asphalt mixes with waste and conventional mineral fillers.

The Marshall stability (MS) of a bituminous mixture is the ultimate load achieved at the failure by the specimens, whereas the Marshall flow is the deformation of the specimen that occurred under peak load. Therefore, from an empirical point of view, the Marshall quotient describes the mechanical resistance of the asphalt mixtures to permanent deformation at high temperatures caused by wheel loads. The MS of SF (13.98 kN) and LSD (13.86 kN) was, resultingly, slightly higher with respect to the asphalt mixtures made with OPC (13.74 kN), as shown in Figure 8. The values of MS for FA (12.39 kN), SD (12.93 kN), MD (12.31 kN), BD (12.6 kN), and RHA (10.18 kN), instead, were lower than the one obtained with conventional filler OPC (13.74 kN) at 8.5% content. It can be also observed that the

value of MS increased with the increase in the filler content; therefore, higher a MS value has been observed at 8.5% mineral filler content. All the asphalt mixtures considered, except for the mixes prepared with RHA and MD (4% filler content), presented MS values higher than 10 kN, as prescribed by Indian regulations [45]. Here, it can be also noted that the OPC, LSD, and SF have shown more or less similar behaviors. This demonstrates that SF and LSD can be effectively recycled in asphalt concrete mixes as a replacement for the OPC.

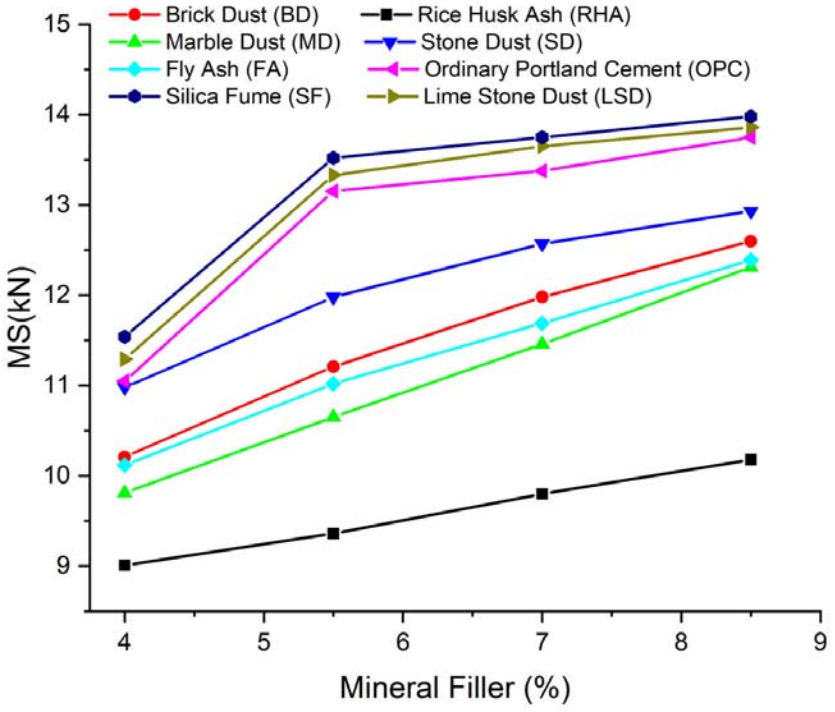

Figure 8. Marshall stability of the asphalt mixes with waste and conventional mineral fillers.

Even the acceptance requisite for mixtures made with modified bitumen (MS higher than 13 kN) is fully satisfied if the filler content is raised from 5.5% to 8.5% in the case of LSD and SF, demonstrating the significant improvement of the mechanical response of the asphalt mixes given by the filler. The Marshall flow of all the asphalt mixes considered were within the range of 2 mm–4 mm, as specified by MoRTH: in particular, the lowest flow values have been observed at 7% and 8.5%. Higher stability, along with a lower flow, is an empirical indicator of an asphalt mixture's resistance against permanent deformations at high temperatures, namely, the rutting phenomenon. The Marshall quotient values of all mixes are specified in Figure 9, and an increasing trend can be observed as the filler content increases. This trend is in agreement with the results obtained in previous studies [19,69]. Figure 9 demonstrates that the Marshall quotient (MQ) values of the SF and LSD filler mixes are higher than those of the OPC mixtures. However, for all the mixtures investigated, the MQ results are within the acceptance range (2 kN/mm–6 kN/mm) of the Indian specifications; hence, the addition of industrial waste does not result in a highly plastic mechanical response, even though the MQ values are lower than OPC for RHA, BPD, SD, MD, and FA.

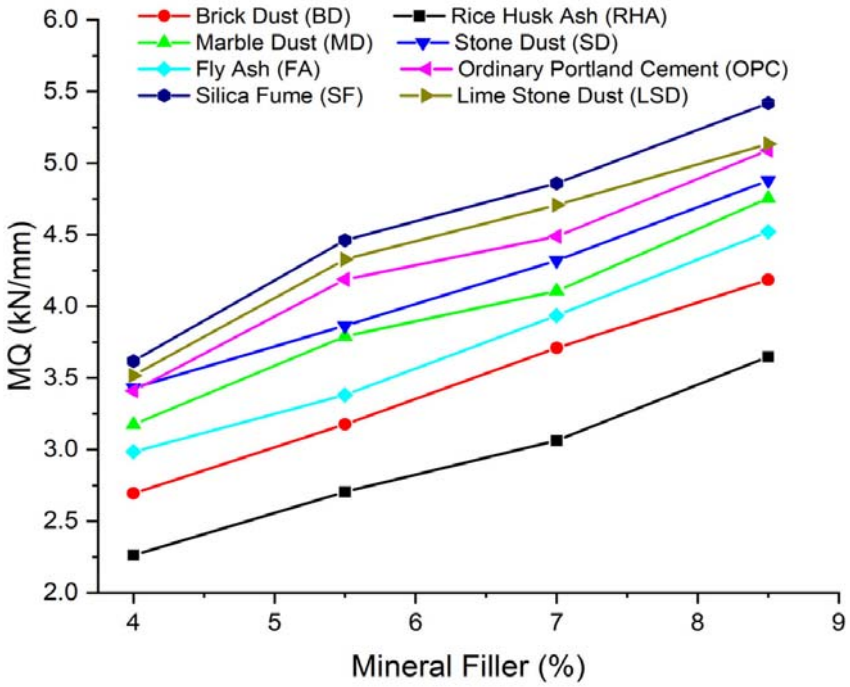

Figure 9. Marshall quotient (kN/mm) of the asphalt mixes with waste and conventional mineral fillers.

3.1.2. Cracking Resistance

The cracking resistance of the asphalt concrete has been assessed with the indirect tensile strength tests. An increase in the ITS values shows a higher resistance of the asphalt concrete against fatigue cracking. The average ITS values for the different filler contents are shown in Figure 10.

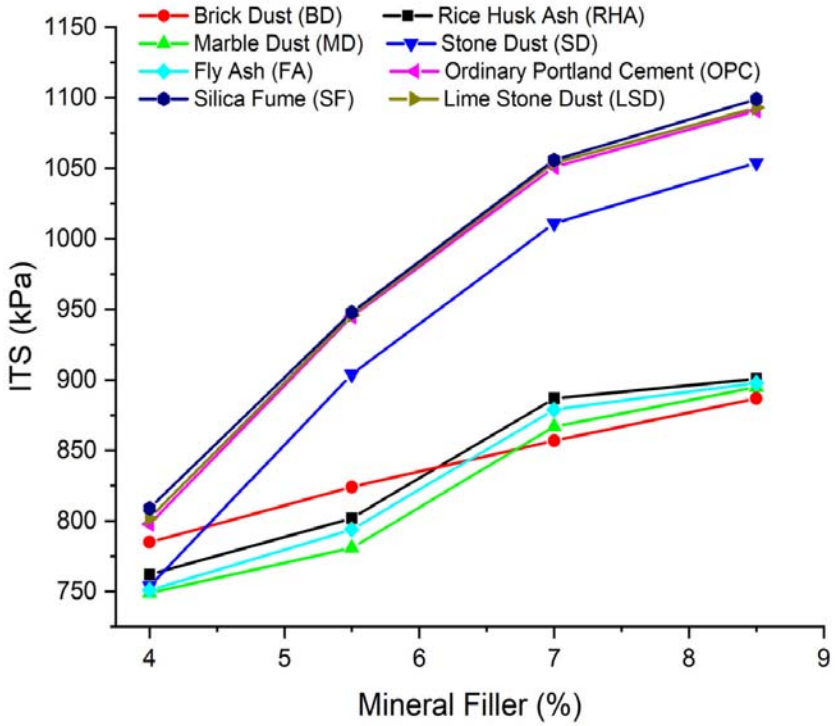

Figure 10. Indirect tensile strength of the asphalt mixes with waste and conventional mineral fillers.

It can be observed that the ITS value of the LSD- and SF-modified asphalt mixture has been improved in comparison to the OPC-modified asphalt concrete. The improvement in the ITS values can be attributed to their higher specific surface area. It can be observed that the ITS values of the LSD- and SF-modified asphalt mixtures were higher than those of the OPC-modified asphalt concretes. It can also be ascertained from the test results that the ITS values of the SD-modified asphalt concretes were closer to those of the OPC-modified asphalt mixes. However, the ITS response of the MD, FA, BD, and RHA mixes was almost similar, but their values were significantly lower than those of the OPC modified mix. Therefore, it can be concluded that the fineness of the mineral filler effectively controls the performance of the asphalt mix. It can also be concluded that the SF and LSD mixes perform almost similar to the OPC mixtures and can suitably replace the OPC in asphalt concrete for the heavy traffic loads. Dehghan and Modarres have verified that fine-mineral fillers with uniform distributions produce an integrated sound structure, and therefore, the ITS values of the asphalt mixes can be improved [70].

3.1.3. Moisture Susceptibility

The moisture susceptibility of the waste filler-modified asphalt concretes is shown in Figure 11. The obtained values have been compared with the OPC-modified asphalt concretes. The moisture susceptibility values have been expressed in terms of ITSR values. As per the Indian standard [45], the ITSR value should be more than 75 %. In all the cases, the waste mineral filler-modified mixtures presented ITSR values above the acceptable limit of moisture susceptibility. The SD-, LSD-, and SF-modified asphalt concretes have demonstrated higher performances than those of the OPC-modified asphalt mixtures. The calcium-based mineral filler performed extremely well due to its higher moisture resistance.

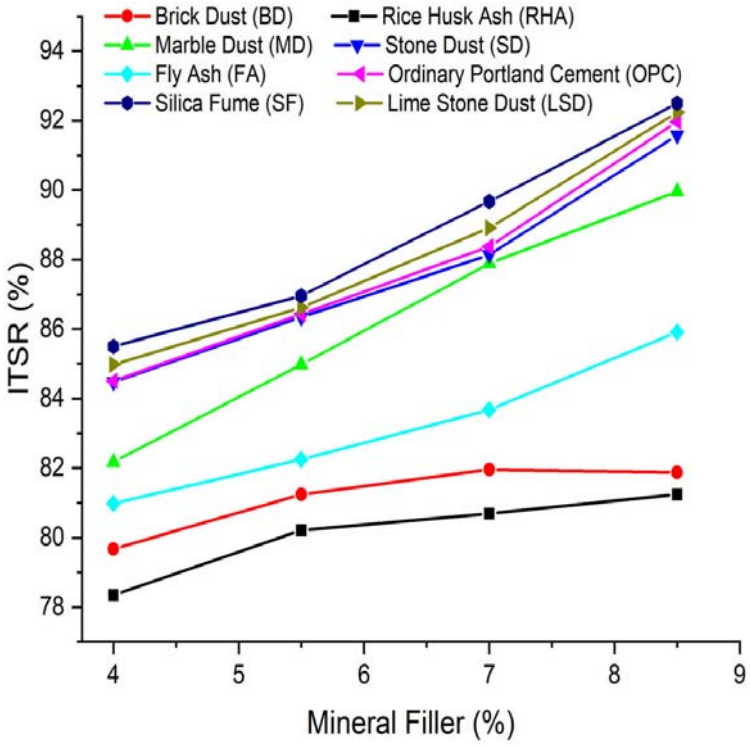

Figure 11. Indirect tensile strength ratio of the asphalt mixes with waste and conventional mineral fillers.

The SF, OPC, SD, and LSD blends exhibited the highest ITSR values. The SF mix had the highest ITSR value due to the presence of portlandite and calcite minerals in its composition. These minerals are primarily constituent of hydrated lime and have antistripping properties. Similarly, LSD has calcite in its composition, which enhances bitumen filler adhesion [51]. This indicates that asphalt mixtures with waste filler SF and

LSD have a better antistripping performance than conventional asphalt mixtures with OPC. The RHA, BD, FA, and MD mixes had lower moisture resistance. The RHA mix had the lowest ITSR value due to the high porosity of RHA. The presence of the fine clays also reduces the performance of the asphalt concrete; therefore, the BPD-modified mixes have shown poor ITSR values. Kuity et al. and Arabani et al. have also shown similar results for the BD-modified asphalt concrete [18,24].

3.1.4. Abrasion Loss

From Figure 12, it can be observed that for all the asphalt mixtures, as the filler content increases, the Cantabro abrasion loss parameter decreases.

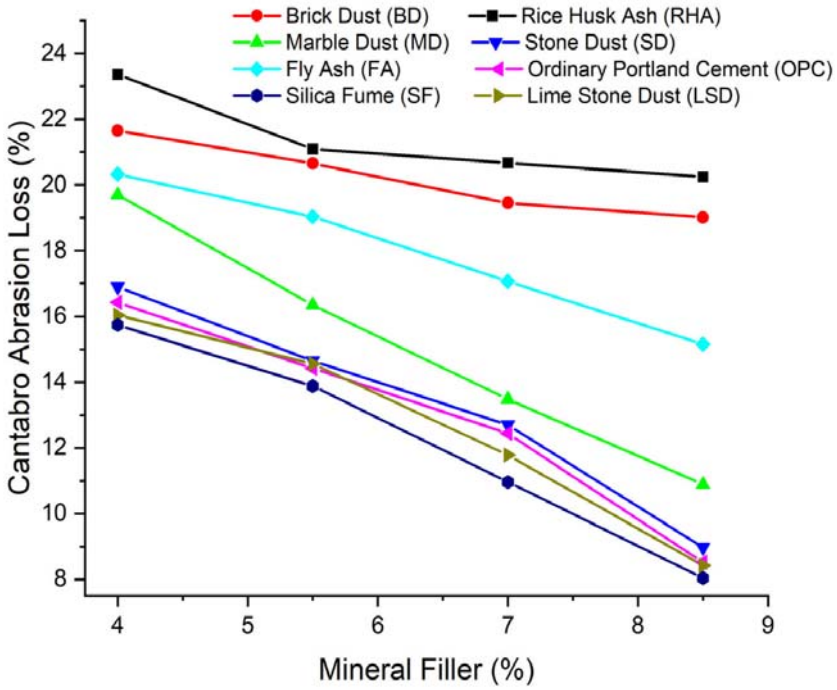

Figure 12. Cantabro abrasion loss of the asphalt mixes with waste and conventional mineral fillers.

Furthermore, mixtures with waste filler SF and LSD perform even better than conventional asphalt mixtures with OPC. The low mass loss rate of the asphalt mix may result from the high cohesion of the filler–bitumen system and the high adhesion at the aggregate–bitumen interface. It has been well reported that the tensile strength and fatigue performance of waste-modified asphalt mixes are much higher than those of conventional asphalt mixes. In fact, a low level of air voids is likely to provide fewer weak points for raveling to occur.

3.2. Numerical Discussion

It is worth reminding the reader that the purpose pursued through the development of a predictive model is to provide road construction companies and/or civil engineers with a tool capable of producing reliable predictions of the asphalt concretes' mechanical behavior, based on their composition and physical properties, avoiding recourse to new laboratory experiments (sometimes time-consuming and costly) when unforeseen events occur during the construction of a road pavement or when different design solutions are to be compared. A model cannot be derived from the simple interpolation of data, as this mathematical operation is not able to capture the semantics of data and to properly identify the complex relationship between them.

Regarding the neural network modeling, the results obtained from the implementation of the k-folds resampling and MAKIMA data-augmentation methods in the SNNs learning

process were satisfactory, considering the small number of experimental observations available. Figure 13 shows graphically the predictive accuracy metrics, averaged over the four test folds of the neural models obtained for each pair $(N,\ \varphi)$. In red, the optimal SNNs for each activation function are marked.

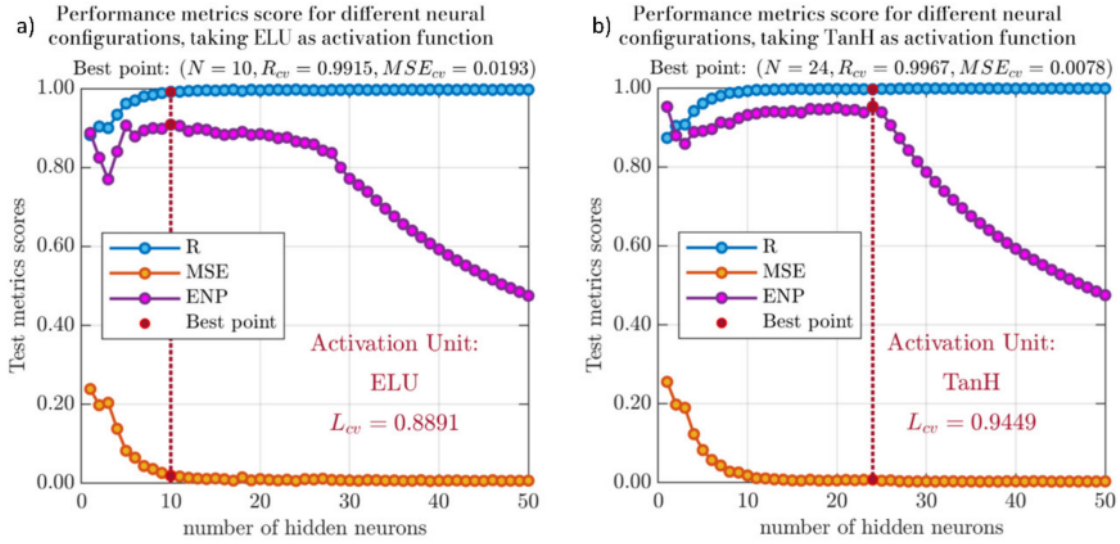

Figure 13. Grid search results with (**a**) ELU as the activation function and with (**b**) TanH as the activation function. In these plots, the results for the correlation coefficient R_{cv} are represented with blue dots, the mean squared error MSE_{cv} with in orange dots, and the effective number of parameters ENP, obtained by testing different possible neural configurations, in purple dots. The red dots identify the optimal solutions for each activation function considered.

It is worth pointing out that the two activation functions considered in this study lead to neural configurations with different efficiency and accuracy levels. In fact, the use of the ELU unit, very common in computer vision problems, results in a compact neural configuration (only $N = 10$ hidden neurons) that is computationally efficient but characterized by a lower), although satisfactory, accuracy ($R_{cv} = 0.9915$ and $MSE_{cv} = 0.0193$) than its counterpart; in fact, the hyperbolic tangent function allows for a better interpretation of the non-linearity problem, leading to the identification of the optimal model ($R_{cv} = 0.9967$ and $MSE_{cv} = 0.0078$). Therefore, the latter is hereafter referred to as SNN_{OPT}. Nevertheless, the better accuracy requires more computational power; the use of $N = 24$ neurons in the hidden layer makes the structure complex and the calculation slightly more onerous than the best ELU network solution. In addition, it should be noted that the $\delta = 196$ parameters (weights and biases) defining the SNN_{OPT} contribute $ENP = 95.27\%$ to define the model's predictive capacity, whereas this value is reduced to 90.84% in the case of ELU function use. Once the optimal solutions for each activation function have been reached, the ENP value begins to gradually decrease (purple dots in Figure 13), indicating that adding any new parameters to the model does not result in a significant improvement in its predictive accuracy, but rather forces the regularization algorithm to minimize the effect of the added parameters. Conversely, it can be observed that the solutions preceding the optimal SNN models (red dots in Figure 12) are progressively improving in performance as the number of hidden neurons increases.

To summarize, the highest score on the objective function L_{CV} (equal to 0.9449, Figure 11) was achieved by the neural configuration defined by $N = 24$ hidden neurons and the $\varphi =$ TanH activation function. This means that the best SNN for the modeling problem in question presents a 3–24–4 architecture. The input layer consists of a neuron for every input feature (the air voids property, the filler content, and the categorical variable distinguishing the filler type). These are connected to 24 processing units in the hidden layer, which, in turn, is characterized by the non-linear activation function TanH. Finally,

the output of each hidden neuron is passed to the four-neuron output layer that, by means of the linear activation function, provides the prediction of the asphalt concrete mechanical parameters. The SNN_{OPT} has very good generalization capability (Figure 12), as the coefficient $R_{cv} = 0.9967$ is so high as to be representative of an almost perfect fit to the experimental data (and, consequently, the normalized $MSE_{cv} = 0.0078$ is actually small). This is not to say that the model is overfitted if the trend of the data requires passing over experimentally sampled points. Figure 14 shows the experimental observations (the dots) and the SNN_{OPT} predictions of the four mechanical parameters (the curves) for each of the eight filler types considered in the study (indicated by eight different colors), according to the filler content vs. air voids relationship curves presented in Figure 5. The analysis of these graphs qualitatively confirms what was pointed out in the experimental discussion: the SNN_{OPT} model is a smooth regression of the experimental observations and does not have any excessive fluctuations or strange oscillations typical of the overfitting phenomenon. Indeed, it is able to preserve and properly reproduce the physical behavior of asphalt concretes. In particular, as the percentage of filler by volume of the mix increases (and consequently, according to the curves in Figure 4, as the air void content decreases), all mechanical features are improved, whatever the type of filler is used.

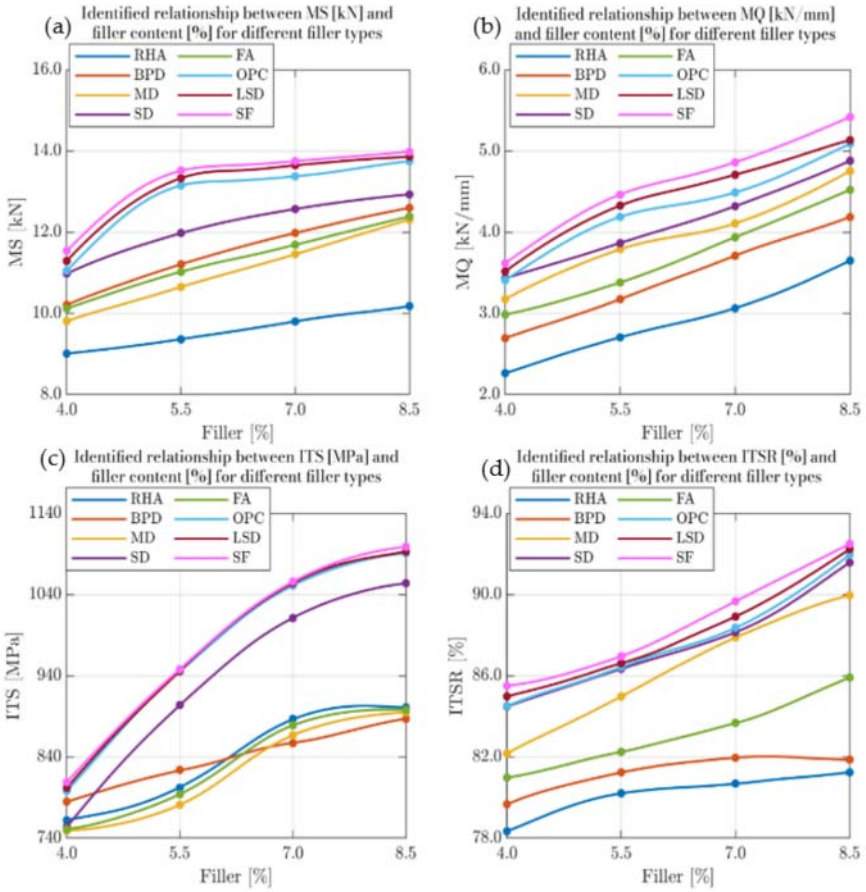

Figure 14. Model prediction vs. experimentally observed target for each filler type: (**a**) MS, (**b**) MQ, (**c**) ITS, and (**d**) ITSR. These plots show the fit of the model to the experimental data and allow the modeling result to be interpreted in physical terms, to verify its correspondence to real-world scenarios.

4. Conclusions

This study investigated the effect of seven different industrial wastes in order to improve the mechanical property of asphalt concrete. A detailed experimental assessment has been carried out to develop the comparative evaluation of the mixes with different fillers in similar conditions. Further, the ANN model is developed to predict the performance of

the asphalt concrete. Based on the detailed experimental and machine learning assessment, the following conclusions are drawn:

1. The chemical and physical properties of silica fume (SF), limestone dust (LSD), stone dust (SD), rice husk ash (RHA), fly ash (FA), brick dust (BD), and marble dust (MD) have been assessed, and it has been observed that all the fillers follow the required requisites of the Indian Standard. Therefore, these fillers can be used in asphalt concrete;
2. The mechanical strength and moisture susceptibility tests on the waste-modified asphalt mixtures have shown satisfactory results with respect to the acceptance requisites, as per the MoRTH. Therefore, these mineral fillers can be effectively used for field applications. The acceptance requisite for mixtures made with modified bitumen (MS higher than 13 kN) is fully satisfied if the filler content is raised from 5.5% to 8.5% in case of LSD and SF, demonstrating the significant improvement to the mechanical response of the asphalt mixes given by the filler. It has been observed that LSD- and SF-modified asphalt mixtures have demonstrated superior performance, compared to the OPC-modified asphalt concretes;
3. The LSD and SF can be identified as the best alternatives to the OPC in asphalt concrete, since the performances of these mixes were better than those of the OPC-modified asphalt concretes. The MS of SF (13.98 kN) and LSD (13.86 kN) was slightly higher, with respect to the asphalt mixtures made with OPC (13.74 kN). The calcium-based mineral filler performed extremely well due to its higher moisture resistance, though the other filler-modified mixtures also fulfilled the requirements of the MoRTH, since ITSR values greater than 75%, and MS values greater than 10 kN have been observed;
4. Shallow neural networks have been successfully used to develop a predictive model of the main empirical and rational mechanical characteristics of ACs prepared with different filler types, namely, Marshall stability (kN), Marshall quotient (kN/mm), indirect tensile strength (kPa), and indirect tensile strength ratio (%);
5. The results obtained from the implementation of the k-folds resampling and MAKIMA data-augmentation methods in the SNN's learning process were fully satisfactory considering the small number of experimental observations available. The optimal SNN for the modeling problem in question receives as input a three-component features vector, the air voids content (%), the filler content (% by volume of the mix), along with the categorical variable distinguishing the filler type; such features are processed by a twenty-four-neuron hidden layer characterized by the hyperbolic tangent activation function;
6. The optimal SNN model is a smooth regression of the experimental observations and is able to properly reproduce the physical behavior of asphalt concretes: as the percentage of filler by volume of the mix increases and, consequently, as the air voids content decreases, all mechanical features are improved, regardless of the type of filler used;
7. The optimal model developed in this study admits solutions only along the univocal relationship existing between the filler content and air voids, as the type and content of bitumen, as well as the type of coarse aggregate, have been kept constant in the preparation of the investigated mixtures. Therefore, this SNN represents a modeling experience that, for the obtained results, encourages the development of an extensive model that can be applied to other types of mixtures and allow the optimal filler contents for each asphalt concrete in question to be properly identified.

For future research, in order to make use of these fillers in the field, this research is required to be expanded by conducting the rutting and fatigue analyses. All the experiments have been conducted at the laboratory scale; therefore, to understand the field behavior, an accelerated pavement test (APT) can be conducted by incorporating the IoT-enabled sensors system. The long-term performance under cyclic loading and the data obtained from APT using IoT sensors can also be used for developing a robust prediction model considering a large dataset. The use of the Bayesian method in order to improve the optimization of the hyperparameters of the ANN model, such as the number of artificial neurons in the hidden layer and the type of transfer function, is recommended.

Author Contributions: Conceptualization, N.T., N.B., N.S. and M.M.; methodology, N.T.; software, M.M.; validation, N.T., N.B. and M.M.; formal analysis, N.T., N.B., N.S. and M.M.; investigation, N.T.; writing—original draft preparation, N.T. and M.M.; writing—review and editing, N.B. and N.S.; supervision, N.S. and N.B. All authors have read and agreed to the published version of the manuscript.

Funding: This research received no external funding.

Institutional Review Board Statement: Not applicable.

Informed Consent Statement: Not applicable.

Data Availability Statement: Not applicable.

Acknowledgments: We are grateful to Sophisticated Instrumentation Centre (SIC), Indian Institute of Technology, Indore, for providing the material characterization facility, and to the Road Lab of the Polytechnic Department of Engineering and Architecture (DPIA), University of Udine, for providing the numerical processing facility. We are thankful the MDPI for providing a full APC waiver for this publication.

Conflicts of Interest: The authors declare no conflict of interest.

References

1. UNFCCC. The Paris Agreement. Available online: https://unfccc.int/process-and-meetings/the-paris-agreement/the-paris-agreement (accessed on 4 April 2022).
2. UNFCCC. Action on Climate and SDGs. Available online: https://unfccc.int/topics/action-on-climate-and-sdgs/action-on-climate-and-sdgs (accessed on 4 April 2022).
3. Choudhary, J.; Kumar, B.; Gupta, A. Utilization of Solid Waste Materials as Alternative Fillers in Asphalt Mixes: A Review. *Constr. Build. Mater.* **2020**, *234*, 117271. [CrossRef]
4. Mohammadhosseini, H.; Tahir, M.M.; Mohd Sam, A.R.; Abdul Shukor Lim, N.H.; Samadi, M. Enhanced Performance for Aggressive Environments of Green Concrete Composites Reinforced with Waste Carpet Fibers and Palm Oil Fuel Ash. *J. Clean. Prod.* **2018**, *185*, 252–265. [CrossRef]
5. Pasetto, M.; Baldo, N. Electric arc furnace steel slags in "high performance" asphalt mixes: A laboratory characterisation. In Proceedings of the MS Fall Extraction and Processing Division: Sohn International Symposium, San Diego, CA, USA, 27–31 August 2006.
6. Pasetto, M.; Baldo, N. Comparative performance analysis of bituminous mixtures with EAF steel slags: A laboratory evaluation. In Proceedings of the 2008 Global Symposium on Recycling, Waste Treatment and Clean Technology, REWAS 2008, Cancun, Mexico, 12–15 October 2008; pp. 565–570.
7. Pasetto, M.; Baldo, N. Recycling of steel slags in road foundations. *Environ. Eng. Manag. J.* **2010**, *9*, 773–777. [CrossRef]
8. Kong, D.; Wu, S.; Chen, M.; Zhao, M.; Shu, B. Characteristics of Different Types of Basic Oxygen Furnace Slag Filler and its Influence on Properties of Asphalt Mastic. *Materials* **2019**, *12*, 4034. [CrossRef]
9. Terrones-Saeta, J.M.; Suárez-Macías, J.; Iglesias-Godino, F.J.; Corpas-Iglesias, F.A. Evaluation of the Use of Electric Arc Furnace Slag and Ladle Furnace Slag in Stone Mastic Asphalt Mixes with Discarded Cellulose Fibers from the Papermaking Industry. *Metals* **2020**, *10*, 1548. [CrossRef]
10. Kang, G.-O.; Kang, J.-G.; Kim, J.-Y.; Kim, Y.-S. Time-Dependent Strength Behavior, Expansion, Microstructural Properties, and Environmental Impact of Basic Oxygen Furnace Slag-Treated Marine-Dredged Clay in South Korea. *Sustainability* **2021**, *13*, 5026. [CrossRef]
11. Gobetti, A.; Cornacchia, G.; Ramorino, G. Innovative Reuse of Electric Arc Furnace Slag as Filler for Different Polymer Matrixes. *Minerals* **2021**, *11*, 832. [CrossRef]
12. Sas, W.; Dzięcioł, J.; Radzevičius, A.; Radziemska, M.; Dapkienė, M.; Šadzevičius, R.; Skominas, R.; Głuchowski, A. Geotechnical and Environmental Assessment of Blast Furnace Slag for Engineering Applications. *Materials* **2021**, *14*, 6029. [CrossRef]
13. Dzięcioł, J.; Radziemska, M. Blast Furnace Slag, Post-Industrial Waste or Valuable Building Materials with Remediation Potential? *Minerals* **2022**, *12*, 478. [CrossRef]
14. Huang, B.; Shu, X.; Chen, X. Effects of Mineral Fillers on Hot-Mix Asphalt Laboratory-Measured Properties. *Int. J. Pavement Eng.* **2007**, *8*, 1–9. [CrossRef]
15. Vavrik, W.R.; Pine, W.J.; Carpenter, S.H. Aggregate Blending for Asphalt Mix Design Bailey Method. *Transp. Res. Rec.* **2002**, *1789*, 146–153. [CrossRef]
16. Wang, H.; Al-Qadi, I.L.; Faheem, A.F.; Bahia, H.U.; Yang, S.H.; Reinke, G.H. Effect of Mineral Filler Characteristics on Asphalt Mastic and Mixture Rutting Potential. *Transp. Res. Rec.* **2011**, *2208*, 33–39. [CrossRef]
17. Tiwari, N.; Satyam, N. Evaluation of Strength and Water Susceptibility Performance of Polypropylene Fiber-Reinforced and Silica Fume-Modified Hot Mix Asphalt. *Adv. Civ. Eng. Mater.* **2021**, *10*, 380–395. [CrossRef]
18. Arabani, M.; Tahami, S.A.; Taghipoor, M. Laboratory Investigation of Hot Mix Asphalt Containing Waste Materials. *Road Mater. Pavement Des.* **2017**, *18*, 713–729. [CrossRef]

19. Chandra, S.; Choudhary, R. Performance Characteristics of Bituminous Concrete with Industrial Wastes as Filler. *J. Mater. Civ. Eng.* **2013**, *25*, 1666–1673. [CrossRef]
20. Woszuk, A.; Bandura, L.; Franus, W. Fly Ash as Low Cost and Environmentally Friendly Filler and Its Effect on the Properties of Mix Asphalt. *J. Clean. Prod.* **2019**, *235*, 493–502. [CrossRef]
21. Xu, P.; Chen, Z.; Cai, J.; Pei, J.; Gao, J.; Zhang, J.; Zhang, J. The Effect of Retreated Coal Wastes as Filler on the Performance of Asphalt Mastics and Mixtures. *Constr. Build. Mater.* **2019**, *203*, 9–17. [CrossRef]
22. Lukjan, A.; Iyaruk, A.; Somboon, C. Evaluation on Mechanical Deterioration of the Asphalt Mixtures Containing Waste Materials When Exposed to Corrosion Solutions. *Int. J. Eng. Technol.* **2022**, *12*, 130–144. [CrossRef]
23. Choudhary, J.; Kumar, B.; Gupta, A. Feasible Utilization of Waste Limestone Sludge as Filler in Bituminous Concrete. *Constr. Build. Mater.* **2020**, *239*, 117781. [CrossRef]
24. Kuity, A.; Jayaprakasan, S.; Das, A. Laboratory Investigation on Volume Proportioning Scheme of Mineral Fillers in Asphalt Mixture. *Constr. Build. Mater.* **2014**, *68*, 637–643. [CrossRef]
25. Choudhary, J.; Kumar, B.; Gupta, A. Performance Evaluation of Bauxite Residue Modified Asphalt Concrete Mixes. *Eur. J. Environ. Civ. Eng.* **2019**, *26*, 978–994. [CrossRef]
26. Modarres, A.; Alinia Bengar, P. Investigating the Indirect Tensile Stiffness, Toughness and Fatigue Life of Hot Mix Asphalt Containing Copper Slag Powder. *Int. J. Pavement Eng.* **2019**, *20*, 977–985. [CrossRef]
27. Awed, A.M.; Tarbay, E.W.; El-Badawy, S.M.; Azam, A.M. Performance characteristics of asphalt mixtures with industrial waste/by-product materials as mineral fillers under static and cyclic loading. *Road Mat. Pavement Des.* **2022**, *23*, 335–357. [CrossRef]
28. Hamedi, G.H.; Esmaeeli, M.R.; Najafi Moghaddam Gilani, V.; Hosseinian, S.M. The effect of aggregate-forming minerals on thermodynamic parameters using surface free energy concept and its relationship with the moisture susceptibility of asphalt mixtures. *Adv. Civ. Eng.* **2021**, *2021*, 8818681. [CrossRef]
29. Sherre, T.K.; Liao, M.C. Characteristics of Recycled Mineral Fillers and Their Effects on the Mechanical Properties of Hot-Mix Asphalt When Used as Limestone Filler Replacements. *J. Mater. Civ. Eng.* **2022**, *34*, 04021395. [CrossRef]
30. Sholevar, N.; Golroo, A.; Esfahani, S.R. Machine learning techniques for pavement condition evaluation. *Autom. Constr.* **2022**, *136*, 104190. [CrossRef]
31. Hou, Y.; Li, Q.; Zhang, C.; Lu, G.; Ye, Z.; Chen, Y.; Wang, L.; Cao, D. The state-of-the-art review on applications of intrusive sensing, image processing techniques, and machine learning methods in pavement monitoring and analysis. *Engineering* **2021**, *7*, 845–856. [CrossRef]
32. Pasetto, M.; Baldo, N. Numerical visco-elastoplastic constitutive modelization of creep recovery tests on hot mix asphalt. *J. Traffic Transp. Eng.* **2016**, *3*, 390–397. [CrossRef]
33. De Oliveira Junior, M.; De Farias, M.M. A simple numerical methodology to simulate creep and recovery tests in HMA. *Constr. Build. Mater.* **2020**, *262*, 120793. [CrossRef]
34. Cao, P.; Leng, Z.; Shi, F.; Zhou, C.; Tan, Z.; Wang, Z. A novel visco-elastic damage model for asphalt concrete and its numerical implementation. *Constr. Build. Mater.* **2020**, *264*, 120261. [CrossRef]
35. Sun, B.; Hao, P.; Zhang, H.; Liu, J. Establishment and verification of a developed viscoelastic damage model and creep instability criterion for modified fine asphalt mortar. *Mater. Struct.* **2022**, *55*, 107. [CrossRef]
36. Hoang, N.D.; Nguyen, Q.L. A novel method for asphalt pavement crack classification based on image processing and machine learning. *Eng. Comput.* **2019**, *35*, 487–498. [CrossRef]
37. Fathi, A.; Mazari, M.; Saghafi, M.; Hosseini, A.; Kumar, S. Parametric study of pavement deterioration using machine learning algorithms. In *Airfield and Highway Pavements 2019: Innovation and Sustainability in Highway and Airfield Pavement Technology*; American Society of Civil Engineers: Reston, VA, USA, 2019; pp. 31–41.
38. Majidifard, H.; Adu-Gyamfi, Y.; Buttlar, W.G. Deep machine learning approach to develop a new asphalt pavement condition index. *Constr. Build. Mater.* **2020**, *247*, 118513. [CrossRef]
39. Marcelino, P.; De Lurdes Antunes, M.; Fortunato, E.; Gomes, M.C. Machine learning approach for pavement performance prediction. *Int. J. Pavement Eng.* **2021**, *22*, 341–354. [CrossRef]
40. Zeiada, W.; Dabous, S.A.; Hamad, K.; Al-Ruzouq, R.; Khalil, M.A. Machine learning for pavement performance modelling in warm climate regions. *Arab. J. Sci. Eng.* **2020**, *45*, 4091–4109. [CrossRef]
41. Gilani, V.N.M.; Hosseinian, S.M.; Behbahani, H.; Hamedi, G.H. Prediction and pareto-based multi-objective optimization of moisture and fatigue damages of asphalt mixtures modified with nano hydrated lime. *Constr. Build. Mater.* **2020**, *261*, 120509. [CrossRef]
42. Behbahani, H.; Hamedi, G.H.; Gilani, V.N.M. Predictive model of modified asphalt mixtures with nano hydrated lime to increase resistance to moisture and fatigue damages by the use of deicing agents. *Constr. Build. Mater.* **2020**, *265*, 120353. [CrossRef]
43. Tapkin, S.; Çevik, A.; Uşar, Ü. Prediction of Marshall Test Results for Polypropylene Modified Dense Bituminous Mixtures Using Neural Networks. *Expert Syst. Appl.* **2010**, *37*, 4660–4670. [CrossRef]
44. Baldo, N.; Manthos, E.; Pasetto, M. Analysis of the Mechanical Behaviour of Asphalt Concretes Using Artificial Neural Networks. *Adv. Civ. Eng.* **2018**, *2018*, 1650945. [CrossRef]
45. Ministry of Road Transport and Highways (MoRTH) India. *Specifications for Road and Bridges Works V*; Ministry of Transport, Department of Surface Transport: New Delhi, India, 2013; Volume 1.

46. *IS 8112-2013*; Ordinary Portland Cement, 43 Grade—Specification. Bureau of Indian Standard: New Delhi, India, 2013.
47. Kandhal, P.S.; Lynn, C.Y.; Parker, F. Characterization Tests for Mineral Fillers Related to Performance of Asphalt Paving Mixtures. *Transp. Res. Rec. J. Transp. Res. Board* **1998**, *1638*, 101–110. [CrossRef]
48. Sousa, J.B.; Way, G.; Harvey, J.T.; Hines, M. Comparison of Mix Design Concepts. *Transp. Res. Rec.* **1995**, *1492*, 151–160.
49. Xue, Y.; Hou, H.; Zhu, S.; Zha, J. Utilization of Municipal Solid Waste Incineration Ash in Stone Mastic Asphalt Mixture: Pavement Performance and Environmental Impact. *Constr. Build. Mater.* **2009**, *23*, 989–996. [CrossRef]
50. Baldo, N.; Manthos, E.; Miani, M. Stiffness Modulus and Marshall Parameters of Hot Mix Asphalts: Laboratory Data Modeling by Artificial Neural Networks Characterized by Cross-Validation. *Appl. Sci.* **2019**, *9*, 3502. [CrossRef]
51. Pasandín, A.R.; Pérez, I. Overview of Bituminous Mixtures Made with Recycled Concrete Aggregates. *Constr. Build. Mater.* **2015**, *74*, 151–161. [CrossRef]
52. Salam Al-Ammari, M.A.; Jakarni, F.M.; Muniandy, R.; Hassim, S. The Effect of Aggregate and Compaction Method on the Physical Properties of Hot Mix Asphalt. In Proceedings of the IOP Conference Series: Materials Science and Engineering, Selangor, Malaysia, 6–8 November 2019; Volume 512.
53. Ozgan, E. Artificial Neural Network Based Modelling of the Marshall Stability of Asphalt Concrete. *Expert Syst. Appl.* **2011**, *38*, 6025–6030. [CrossRef]
54. Zavrtanik, N.; Prosen, J.; Tušar, M.; Turk, G. The Use of Artificial Neural Networks for Modeling Air Void Content in Aggregate Mixture. *Autom. Constr.* **2016**, *63*, 155–161. [CrossRef]
55. *ASTM D6927-15*; Standard Test Method for Marshall Stability and Flow of Asphalt Mixtures: Designation: D6927-15. ASTM International: West Conshohocken, PA, USA, 2015; Volume I.
56. Zoorob, S.E.; Suparma, L.B. Laboratory Design and Investigation of the Properties of Continuously Graded Asphaltic Concrete Containing Recycled Plastics Aggregate Replacement (Plastiphalt). *Cem. Concr. Compos.* **2000**, *22*, 233–242. [CrossRef]
57. *ASTM D6931−17*; Standard Test Method for Indirect Tensile (IDT) Strength of Asphalt Mixtures. ASTM International: West Conshohocken, PA, USA, 2017.
58. Aschenbrener, T.; Mcgennis, R.B. *Investigation of the Modified Lottman Test to Predict the Stripping Performance of Pavements in Colorado*; Final Report; U.S. Department of Transportation Federal Highway of Administration: Washington, DC, USA, 1993.
59. *AASHTO(T-283)*; Standard Method of Test for Resistance of Compacted Asphalt Mixtures to Moisture Induced Damage. American Association of State Highway and Transportation Officials (AASHTO): Washington, DC, USA, 2014.
60. *TxDOT: Tex-245-F*; Test Procedure for Cantabro Loss. Materials and Test Division Texas Department of Transportation: Austin, TX, USA, 2019.
61. Widrow, B.; Hoff, M.E. *Adaptive Switching Circuits*; IRE WESCON Convention Record Part 4; Institute of Radio Engineers: New York, NY, USA, 1960.
62. McCulloch, W.S.; Pitts, W. A Logical Calculus of the Ideas Immanent in Nervous Activity. In *Neurocomputing: Foundations of Research*; Anderson, J.A., Rosenfeld, E., Eds.; The MIT Press: Cambridge, MA, USA, 1998; pp. 15–27.
63. Hagan, M.T.; Demuth, H.B.; Beale, M.H.; De Jesus, O. *Neural Network Design*, 2nd ed.; PWS Publishing Co.: Worcester, UK, 2014; ISBN 1846283027.
64. Hagan, M.T.; Menhaj, M.B. Training Feedforward Networks with the Marquardt Algorithm. *IEEE Trans. Neural Netw.* **1994**, *5*, 989–993. [CrossRef]
65. MacKay, D.J.C. Bayesian Interpolation. *Neural Comput.* **1992**, *4*, 415–447. [CrossRef]
66. Akima, H. A Method of Bivariate Interpolation and Smooth Surface Fitting Based on Local Procedures. *Commun. ACM* **1974**, *17*, 18–20. [CrossRef]
67. Oh, C.; Han, S.; Jeong, J. Time-Series Data Augmentation Based on Interpolation. *Procedia Comput. Sci.* **2020**, *175*, 64–71. [CrossRef]
68. Kutuk-Sert, T. Stability Analyses of Submicron-Boron Mineral Prepared by Mechanical Milling Process in Concrete Roads. *Constr. Build. Mater.* **2016**, *121*, 255–264. [CrossRef]
69. Smith, B.J. Low-Temperature and Dynamic Fatigue Toughening Mizchanisms in Asphalt Mastics and Mixtures. Ph.D. Thesis, Queen's University, Kingston, ON, Canada, 2000.
70. Dehghan, Z.; Modarres, A. Evaluating the Fatigue Properties of Hot Mix Asphalt Reinforced by Recycled PET Fibers Using 4-Point Bending Test. *Constr. Build. Mater.* **2017**, *139*, 384–393. [CrossRef]